Flytzani-Stephanopoulos M. Low-temperature water–gas shift reaction over Cu- and Ni-loaded cerium oxide catalysts

Article *in* Applied Catalysis B Environmental · August 2000

Impact Factor: 7.44 · DOI: 10.1016/S0926-3373(00)00147-8

3 authors, including:

Maria Flytzani-stephanopoulos
Tufts University
88 PUBLICATIONS **6,145** CITATIONS

SEE PROFILE

ELSEVIER

Applied Catalysis B: Environmental 27 (2000) 179–191

APPLIED CATALYSIS B: ENVIRONMENTAL

www.elsevier.com/locate/apcatb

Low-temperature water-gas shift reaction over Cu- and Ni-loaded cerium oxide catalysts

Yue Li[1], Qi Fu, Maria Flytzani-Stephanopoulos*

Department of Chemical Engineering, Tufts University, Medford, MA 02155, USA

Received 23 August 1999; received in revised form 29 February 2000; accepted 3 March 2000

Abstract

In this paper we report on the activity of Cu- and Ni-containing cerium oxide catalysts for low-temperature water-gas shift (WGS). Bulk catalysts were prepared in nanocrystalline form by the urea co-precipitation–gelation method. Lanthanum dopant (10 at.%) was used as a structural stabilizer of ceria, while the content of Cu or Ni was in the range of 5–15 at.% (2–8 wt.%). At low metal loadings, Cu or Ni were present in the form of highly dispersed oxide clusters, while at high loadings, clusters as well as particles of CuO or NiO (>10 nm in size) were present on ceria. Both Cu and Ni increased the reducibility of ceria, as evidenced by H_2-TPR experiments. The WGS reaction activity of Ce(La)O_x was increased significantly by addition of a small amount (2 wt.%) of Cu or Ni. The catalysts were not activated prior to testing. Steady-state WGS kinetics were measured over the temperature range of 175–300 and 250–300°C, respectively, for Cu- and Ni–Ce(La)O_x. The activation energy of the reaction over Ce(La)O_x was 58.5 kJ/mol, while it was 38.2 and 30.4 kJ/mol, respectively, over the 5 at.% Ni–Ce(La)O_x and 5 at.% Cu–Ce(La)O_x catalysts in CO-rich conditions. A co-operative redox reaction mechanism, involving oxidation of CO adsorbed on the metal cluster by oxygen supplied to the metal interface by ceria, followed by H_2O capping the oxygen vacancy on ceria, was used to fit the kinetics. Parametric studies were mainly performed with the 5 at.% Cu–(La)O_x catalyst. Notably, this material requires no activation and retains high WGS activity and stability at temperatures up to 600°C.

Keywords: Cerium oxide; Copper oxide; Nickel oxide; Water-gas shift catalysts; Fuel cells; Oxygen storage capacity

1. Introduction

In recent years, there has been a renewed interest in the water-gas shift (WGS) reaction:

$$CO + H_2O \rightarrow CO_2 + H_2$$

$$\Delta H = -41.2\,\text{kJ/mol}, \quad \Delta G = -28.6\,\text{kJ/mol}$$

because of its potential use in conjunction with fuel-cell power generation. The fuel-cell technology, an attractive, energy-efficient process, is currently undergoing rapid development for both power plant and transportation applications. In the transportation sector, fuel cells could replace the internal combustion engine in cars, trucks, buses, etc. and meet the most stringent emission regulations.

Fuel cells directly convert the chemical energy of fuels into electric and thermal energy, without combustion. Unlike thermal engines, their thermodynamic efficiency is not limited by that of a Carnot cycle and is in fact generally much higher than that of thermal

* Corresponding author. Tel.: +1-617-627-3048; fax: +1-617-627-3991.
E-mail address: mstephanopoulos@infonet.tufts.edu (M. Flytzani-Stephanopoulos)
[1] Present address: Prototech Co., Needham, Massachusetts 02194.

0926-3373/00/$ – see front matter
PII: S0926-3373(00)00147-8

engines. Of course, other factors limit the efficiency of the present-generation fuel cells to 40–50%. However, this is still two to three times that of the internal combustion engine of a typical vehicle. Oxygen from the air, plus hydrogen fuel, obtainable from natural gas, gasoline or methanol, combine electrochemically in a fuel cell to produce electricity. Heat and water vapor are the only by-products.

In many practical cases, the hydrogen feedstock will be obtained from hydrogen-rich fuels by on-board reforming. Generally, the reformate gas will include H_2, CO, CO_2, H_2O and a small amount of CH_4. However, the carbon monoxide formed by the reforming reaction needs to be completely converted both because it is a criterion pollutant and also because it poisons the platinum electrodes, thus hampering the fuel-cell performance. WGS is used to convert carbon monoxide with water to hydrogen and CO_2 products. To avoid the use of (expensive) H_2-permeable membranes, 'advanced low-temperature shift catalysts' are needed to supply CO-free hydrogen to the PEM fuel cell. Hence, the renewed interest in the 'mature' WGS process.

Due to its industrial importance, the water-gas shift reaction has been studied extensively [1–8]. For production of high-purity hydrogen, e.g. for ammonia synthesis, the present practice in industry is to carry out the water-gas shift reaction in two distinct stages with two types of catalyst. One is a high-temperature shift catalyst based on iron oxide promoted with chromium oxide, while the other is a low-temperature shift catalyst composed of copper, zinc oxide and alumina [4].

Binary CuO–ZnO and ternary CuO–ZnO–Al_2O_3 and CuO–ZnO–Cr_2O_3 mixed oxide catalysts have been widely employed commercially since the early 1960s in the water-gas shift reaction. They are generally used in low (180–250°C) and mid- temperature (220–350°C) applications of the reaction [2,5]. In these commercial catalyst systems, zinc oxide and/or chromium oxide are generally used as structural stabilizers and promoters. Aluminum oxide, although inactive for the WGS reaction, is added to improve the catalyst dispersion. The typical composition of the catalyst in the unreduced state is: 1 ZnO:0.24 Cr_2O_3:0.24 CuO, with 2–5 wt.% of Mn, Al and Mg oxides [6,7]. Another material recognized since the late 1970s as an industrial, sulfur resistant water-gas shift catalyst, is sulfided cobalt oxide–molybdenum oxide on alumina [9,10].

Gold supported on iron oxide shows WGS activity, as reported recently by Andreeva and co-workers [11,12]. Over 80% conversion of CO was measured at 200°C with gas hourly space velocity (GHSV)=4000 h^{-1} using an Au:Fe=1:22 atomic ratio. These workers have proposed the associative mechanism for the WGS reaction and attributed the catalytic activity to the ability of gold atoms to generate active hydroxyl groups. Sakurai et al. [13] reported that Au deposited on TiO_2, which contains neither copper nor iron oxide, is a novel more active catalyst, exhibiting low-temperature activity both for the forward and the reverse water-gas shift reactions. However, this type of gold catalyst is very sensitive to preparation conditions [14] and requires a large metal loading (∼5%), which makes the catalyst prohibitively expensive for large-scale application.

A very good WGS catalyst is cerium oxide loaded with platinum metals. In fact, WGS activity is one of the main functions of ceria in the automobile three-way catalyst [15–18]. Cerium oxide-based WGS catalysts have attracted increasing attention primarily because of the high oxygen-storage capacity of ceria and modified ceria [19]. In practice, the role of CeO_2 is not limited to storage of oxygen. The picture is much more complicated, with ceria serving as a stabilizer of both the noble metal and alumina, as well as a promoter of several reactions including the water-gas shift and carbon monoxide oxidation.

Weibel et al. [20] studied the WGS kinetics over Rh–CeO_2–Al_2O_3. They described the reaction mechanism as a regenerative one, in which carbon monoxide is inserted into the oxidic species $RhCeO_2$ to give carbon dioxide and an oxygen vacancy, immediately filled by water to give hydrogen. Similar results were obtained recently by Bunluesin and Gorte over ceria-supported Pt, Rh and Pd [21]. Their results demonstrate the importance of oxygen storage capacity and oxygen mobility in this type of catalyst. A redox reaction model, whereby CO adsorbed on the metal is oxidized by ceria, which in turn is oxidized by water, was proposed. The authors noted that the 'ceria-mediated' processes of CO oxidation and water-gas shift appeared to be both controlled by the same two steps, namely: transfer of oxygen from ceria to the metal interface and re-oxidation of ceria [21].

Ample evidence of the redox reaction mechanism is found in oxidation reactions over ceria-supported metal–metal oxides. This is not limited to noble metals on ceria. Our interest in examining ceria-supported Cu and Ni oxides as catalysts for the water-gas shift reaction stems from our recent findings that these base-metal catalysts are very active for carbon monoxide oxidation by O_2 or SO_2, in the latter case producing elemental sulfur and CO_2 [22–27,45]. In his thesis work, Liu found that Cu–CeO_2 was active for WGS at temperatures much lower than CeO_2 alone [22]. More recently, Li [26] studied Cu- and Ni-containing ceria for this reaction. Compared to the binary CuO–ZnO and ternary CuO–ZnO–Al_2O_3(Cr_2O_3) commercial water-gas shift catalysts, CeO_2-based catalysts are expected to exhibit better thermal stability and may, thus, extend the operating temperature range of the catalyst.

In this work, we have studied the water-gas shift reaction over both copper- and nickel-loaded cerium oxide catalysts to further elucidate the properties of these ceria-based materials. The effect of each metal on the ceria reducibility and reactivity was compared. Steady-state kinetics measurements of the WGS reaction were carried out over the temperature range 175–300°C for Cu–ceria and 250–300°C for the Ni–ceria catalysts.

2. Experimental

2.1. Catalyst preparation and characterization

Bulk catalysts were synthesized by the urea co-precipitation–gelation method [28], which we have found to give ceria-based samples a better homogeneity and higher surface area than conventional co-precipitation with ammonium carbonate [29,30]. The precursor salts were metal nitrates (Aldrich, A.C.S. grade). The cerium salt was $(NH_4)_2Ce(NO_3)_6$ (Aldrich, 99.99%). The preparation procedure consists of mixing aqueous metal nitrate solutions with urea (H_2N–CO–NH_2); heating the solution to 100°C under vigorous stirring and addition of de-ionized water; boiling the resulting gel for 8 h at 100°C; filtering and washing the precipitate twice with de-ionized water at 50–70°C; drying the cake in a vacuum oven at 80–100°C for 10–12 h; crushing the dried lump into smaller particles and calcining the powder in a muffle furnace at the desired temperature for a few hours. A heating rate of 2°C/min was used in the calcination step.

Supported catalysts were prepared by incipient wetness impregnation of a ceria support (doped with 10 at.% La) prepared by the urea co-precipitation–gelation method as above. La-doped ceria, designated as Ce(La)O_x throughout this paper, has been found in other work in our lab [28,30] to retain a small crystallite size (7 nm) and medium high surface area (90–110 m^2/g) after calcination at 650°C. After impregnation with an aqueous solution of metal nitrate of volume equal to the pore volume of the support, the sample was dried in a vacuum oven at 80–100°C for 8–12 h and then crushed and calcined in air in a muffle furnace, typically at 650°C for 2–3 h.

The BET surface area of fresh and used samples was measured on a Micromeritics Pulse ChemiSorb 2705 instrument using a 30% N_2–He gas mixture. Bulk elemental composition was determined by inductively coupled plasma (ICP) atomic emission spectrometry (Perkin-Elmer, Plasma 40). The structure and crystal phase composition of the materials were followed by X-ray diffraction (XRD) on a Rigaku 300 instrument.

2.2. Apparatus and procedure

Activity tests were performed at atmospheric pressure with 150 mg catalyst powder (50–150 μm size) loaded on a quartz frit at the center of a flow quartz-tube reactor (1.0 cm ID), which was heated inside an electric furnace. The feed gas mixture typically contained 2 mol% CO and 10.7 mol% H_2O in helium. In some tests, 40 mol% H_2 was also included in the feed gas. The total gas flow rate was 100 cm^3/min (NTP). The corresponding contact time for the ceria-based samples was 0.09 g s/cm^3 (GHSV=80 000 h^{-1}). All ceria samples were used in the as-prepared form without activation. Activation was only applied to a commercial copper catalyst (UCI, G-66A) used in the activity tests for comparison with the Cu–ceria catalyst. Water was injected into the flowing gas stream by a calibrated water pump and vaporized in the heated gas feed line before entering the reactor. A condenser filled with ice was installed at the reactor exit to collect water. The exit gas stream was continuously analyzed for CO_2

by an on-line NDIR CO_2 Analyzer (Beckman Model 864). The gas mixture was also analyzed by a gas chromatograph, HP-5880A, equipped with a thermal conductivity detector and a 1/4 in. Carbosphere column for CO and CO_2 separation.

Reaction rate measurements were conducted in a smaller-diameter quartz tube reactor (0.5 cm ID). The sample particle size was in the range of 50–150 μm, the same as for the activity tests. Separate experiments at various contact times from 0.005 to 0.05 g s/cm^3 (STP) were carried out in order to establish mass transfer-free operating conditions for each temperature. The conversion of CO was kept <15% by adjusting either the amount of catalyst or the total gas flow rate. The carbon dioxide product was used to calculate the reaction rate by

$$\text{Rate} = \frac{N_t \times CO_{2_{out}}}{W_{cat}} \left(\frac{\text{mol}}{\text{g s}}\right)$$

where N_t is the total dry gas molar flow rate in mol/s, $CO_{2_{out}}$ the molar fraction of CO_2 in the product gas stream and W_{cat} represents the catalyst weight in grams.

We investigated the potential correlation of catalyst activity with the reducibility of CuO- or NiO-loaded ceria catalysts by conducting temperature-programmed reduction (TPR) experiments. In this work, TPR of several catalysts, including Ce(La)O_x, 5 at.% Ni–Ce(La)O_x and 15 at.% Cu–Ce(La)O_x, was performed in a Cahn TG 121 Thermogravimetric Analyzer (TGA). A catalyst load of 5 mg was typically used. This was pre-treated in flowing He at 500°C for 30 min followed by cooling to room temperature to get a stable baseline in He. The reducing gas stream of 5% H_2–He was then switched in at a flowrate of 600 cm^3/min (NTP) and reduction began. The temperature was raised to 700°C at a heating rate of 10°C/min. Weight change data with time–temperature were collected and analyzed as such and in a derivatized form.

3. Results and discussion

3.1. Catalyst reactivity and characterization

Fig. 1 shows CO conversions over ceria and Cu- or Ni-containing ceria. Solid lines are data collected at GHSV=80 000 h^{-1}, while the dashed line is for 8000 h^{-1} (NTP). In all tests the CO was converted to CO_2, i.e. no methanation activity was observed over these catalysts. As shown by the shift of the reaction light-off temperature to lower values, both copper and nickel-containing cerium oxide are

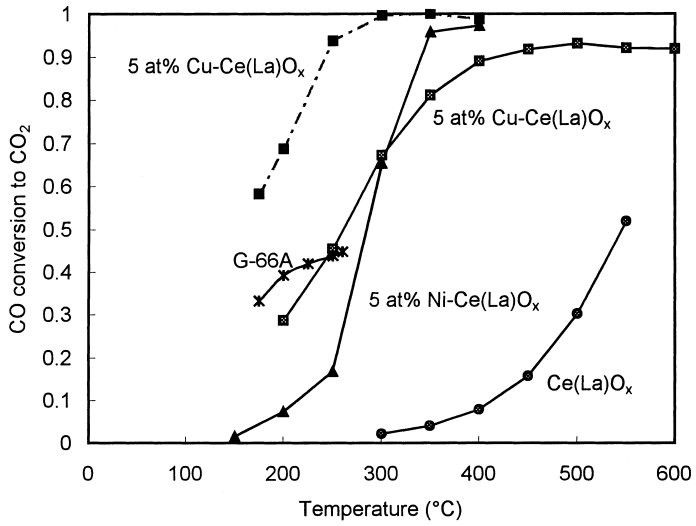

Fig. 1. Water-gas-shift reactivity over several ceria-based catalysts and G-66A (UCI) 2% CO–10.7% H_2O–He, solid lines: S.V.=80 000/h (NTP); dashed line: S.V.=8000 h^{-1} (NTP).

Table 1
BET surface area of catalysts used in this work

Sample	Fresh catalysts[a] (m^2/g)	Used catalysts[b] (m^2/g)
Ce(10% La)O_x[c]	91.7	84.0
5 at.% Ni–Ce(10% La)O_x[c]	94.1	97.1
5 wt.% Ni–Ce(10% La)O_x[d]	65.2	52.9
7 wt.% Ni–Ce(10% La)O_x[d]	69.3	61.1
5 at.% Cu–Ce(10% La)O_x[c]	92.4	90.3
15 at.% Cu–Ce(10% La)O_x[c]	59.6	55.3
40 at.% Cu–Ce(10% La)O_x[c]	46.0	38.9
42 wt.% CuO–47 wt.% ZnO–10 wt.% Al_2O_3[e]	49	–

[a] All samples were calcined in air at 650°C for 3 h.
[b] Used in the water-gas shift reaction with 2% CO–10.7% H_2O–He at temperatures up to 600°C for 18 h.
[c] Prepared by the urea co-precipitation–gelation method [28,26,30].
[d] Prepared by incipient wetness impregnation of Ce(10%La)O_x.
[e] UCI, G-66A; as received, crushed into 50–150 μm size particles.

superior WGS catalysts compared to Ce(La)O_x. Notably, higher than 90% CO conversion was measured at 400°C over the metal oxide-containing ceria, while the corresponding CO conversion over Ce(La)O_x was less than 10% at this temperature. At the low temperature end, the 5 at.% Cu–Ce(La)O_x sample shows similar activity to a commercial Cu–ZnO–Al_2O_3 catalyst (UCI, G-66A), which was used after activation according to the manufacturer-recommended conditions. On the other hand, no activation was necessary for the ceria-based copper catalysts containing a much lower amount of copper (Table 1).

It is interesting to compare these catalysts in terms of their physical properties and structural stability in thermal treatment and in reaction conditions. Generally, bulk ceria catalysts prepared by the urea co-precipitation–gelation method have higher surface area and smaller crystallite size than those prepared by co-precipitation with Na- or NH_4-carbonate [28,30]. This is due to the long boiling step and the slow decomposition of urea, which allows more homogeneous precipitation. A small amount (up to 10 at.%) of Cu or Ni added into cerium oxide had little effect on the surface area compared to the corresponding Ce(La)O_x. This is shown in Table 1 for catalysts calcined in air at 650°C. However, with increasing metal loading, the surface area is typically reduced. This is shown in Table 1 for both the Cu- and Ni-containing ceria samples. On the other hand, after exposure of the 650°C-calcined catalysts to the WGS reaction atmosphere up to 600°C for a total of 14–18 h, very little or no further loss of surface area took place (Table 1). Hence, the data of Fig. 1 were collected under similar and constant surface area for all three ceria-based samples. The surface area of the commercial G-66A catalyst was 49 m^2/g.

XRD patterns of Cu–Ce(La)O_x catalysts prepared by the urea co-precipitation–gelation technique are shown in Fig. 2. In all samples, the distinct fluorite-type oxide structure of CeO_2 was present. Lanthanum is in oxide solid solution with ceria [22,29,31,46], so there are no separate reflections from La-compounds. No CuO reflections are found up to 15 at.% copper content, which is in agreement with previous studies [22,29–31,46]. This may be due to oxide solid solution formation [32] or to the copper phase being finely dispersed in ceria [22,33]. In previous studies, we have demonstrated the existence of highly dispersed copper oxide clusters in ceria by STEM/EDS [22,23,33]. The coexistence of clusters and CuO particles was also shown by distinct TPR peaks [29,30,33]. The fraction of CuO particles increases with copper loading. In Fig. 2, the CuO reflections at $2\theta \approx 35.5$ and 38.8° are seen to increase with the content of Cu (from 15 to 40 at.% Cu).

Fresh and reaction-used samples of 40 at.% Cu–Ce(La)O_x are compared in Fig. 2. In the used sample (up to 600°C), only metallic copper is found by XRD. The CuO particles in this sample are reduced to Cu metal at WGS conditions. It is not clear what happens to the copper clusters, however, which are in close association with the ceria. Stabilization of Cu^{+1}

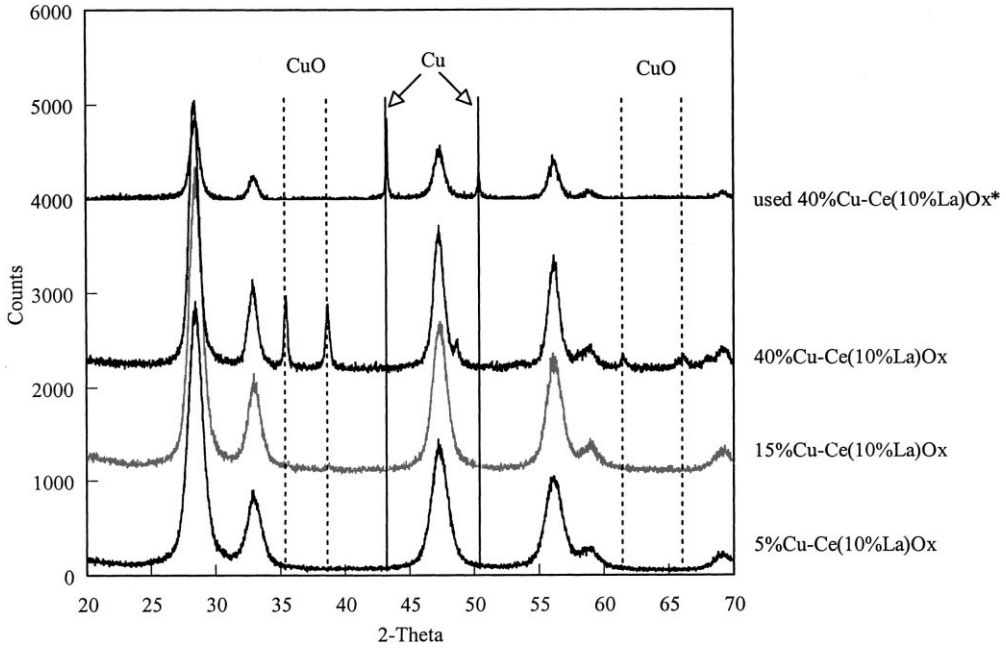

Fig. 2. XRD patterns of Cu–Ce(10% La)O_x catalysts, as-prepared after 650°C calcination; (*) after WGS: 2% CO–10.7% H_2O–He, up to 600°C, 18 h.

is possible, even under hydrogen-rich conditions on this type catalyst [32]. The fluorite-type oxide diffraction pattern of CeO_2 was present in both fresh and used Cu–Ce(La)O_x samples, indicating that ceria is stable in the WGS reaction atmosphere. The presence of Ce^{3+} during reaction is, of course, highly probable, but this cannot be checked by ex situ XRD analysis.

Fig. 3 shows the XRD patterns of fresh and used Ni–Ce(La)O_x samples. No nickel compounds are seen at low Ni loading. The presence of NiO clusters in ceria was identified in recent STEM/EDS work in this lab [31,46]. NiO reflections at $2\theta \approx 37$, 43.7 and 62.9° are present in the 7 wt.% Ni–ceria sample (Fig. 3). In the reaction-used samples, these reflections are absent, while metallic nickel lines are clearly seen. In an XRD study conducted by Barrault et al. [34], only metallic nickel reflections were found in NiO–CeO_2 samples reduced at 250 and 400°C. However, the presence of Ni^{2+} sites in clusters closely associated with ceria cannot be ruled out, as discussed by Lamonier et al. [32].

Temperature-programmed reduction (TPR) by H_2 has been used extensively in the literature to characterize the surface and bulk oxygen reducibility of doped CeO_2 catalysts. Yao and Yu Yao [18] reported that the reduction peaks of the surface capping oxygen and the bulk oxygen of CeO_2 are at 500 and 800°C, respectively. Platinum addition shifted these peaks to considerably lower temperatures [18]. We recently reported that the Cu–CeO_2 system similarly displays enhanced reducibility of ceria [29,30,33]. In turn, ceria affects the reducibility of metal oxides supported on it [22,26,29,30,33,37]. Fierro et al. [35], Boyce et al. [36] and Barrault et al. [34] investigated the TPR profiles of CuO and NiO particles on different supports, such as CeO_2, Al_2O_3 and SiO_2. Bulk CuO is reduced at 200–300°C, while NiO is reduced at 300–400°C.

In this work, TPR was carried out in the TGA with several as-prepared Cu- or Ni–Ce(La)O_x catalysts in powder form (<150 μm size particles) using a gas mixture of 5% H_2–He as the reducing gas. Fig. 4 shows typical TPR plots (in derivatized form) of the weight change of Ce(La)O_x, 5 at.% Ni–Ce(La)O_x and 15 at.% Cu–Ce(La)O_x with temperature. Two reduction peaks were observed for 15% Cu–Ce(La)O_x as can be seen in Fig. 4. The first reduction begins around 120°C with a peak at 150°C, which was previously assigned to

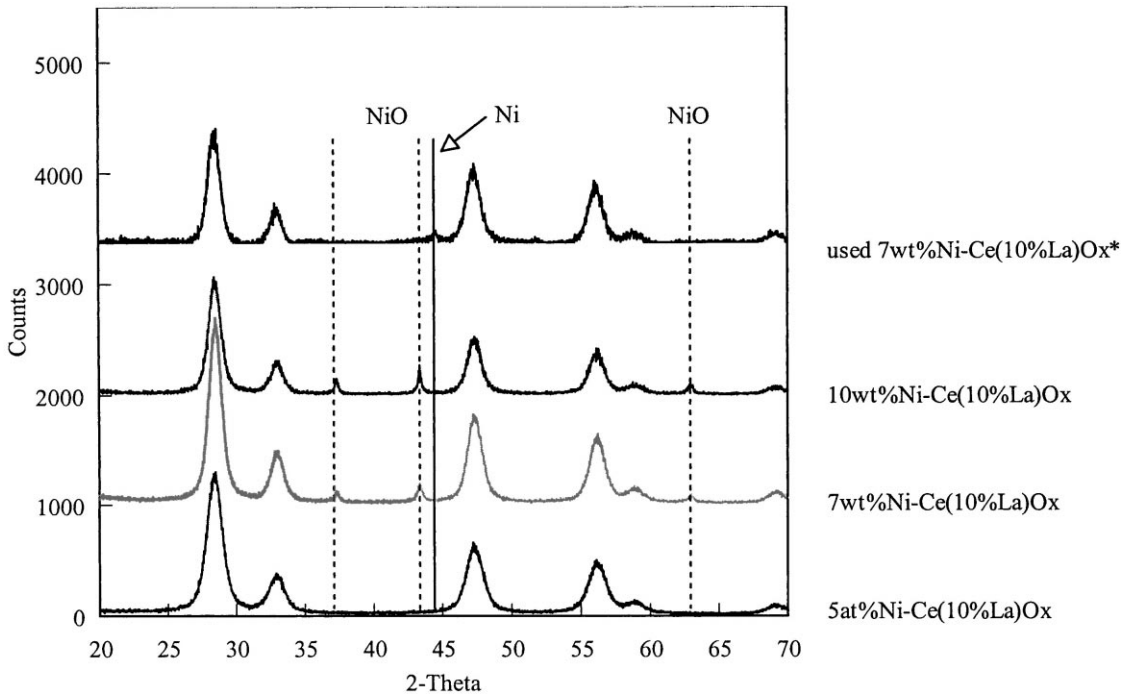

Fig. 3. XRD pattern of Ni–Ce(10% La)O_x catalysts, as-prepared after 650°C calcination; (*) after WGS: 2% CO–10.7% H_2O–He, up to 550°C, 14 h.

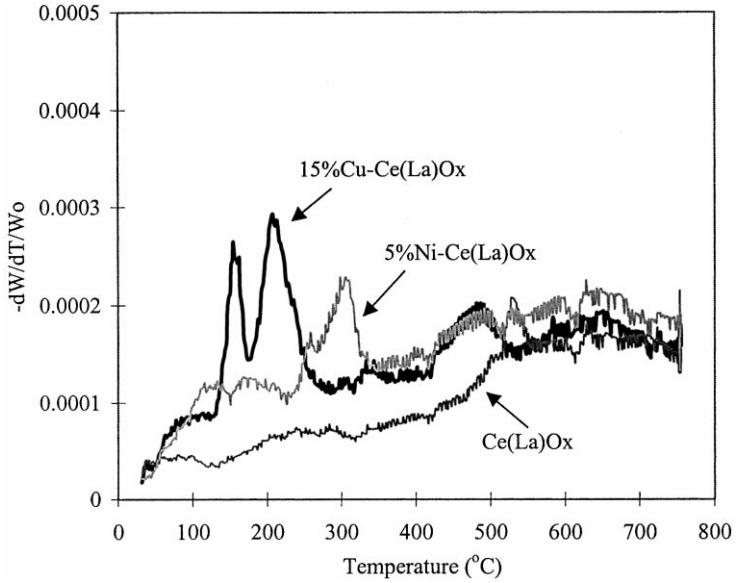

Fig. 4. H_2-TPR profiles of Ce(10% La)O_x and Cu-and Ni-modified Ce(10% La)O_x in 5% H_2/He in the TGA (600 cm^3/min, 10°C/min).

the reduction of copper oxide clusters [22,29,30,33], while the second peak at 200°C is attributed to the reduction of CuO particles. Nickel oxide reduction begins at 220°C with a first peak at 250°C and a second peak at ~300°C. Again, we may assign the first peak to reduction of NiO clusters. The addition of transition metals (Cu, Ni) improves the reducibility of ceria. Reduction of ceria begins below 200°C for 5 at.% Cu–Ce(La)O_x, as also shown in recent work [30] and below 300°C for 5 at.% Ni–Ce(La)O_x [26]. The latter was reported to begin around 400°C for the NiO–CeO_2 system studied by Barrault et al. [34].

3.2. Parametric studies

3.2.1. Effect of contact time

Fig. 1 shows the effect of contact time on the steady-state CO conversion versus temperature profiles over 5 at.% Cu-Ce(La)O_x. Better than 90% CO conversion to CO_2 was achieved at 250°C with a contact time of 0.9 g s/cm^3 (NTP), corresponding GHSV=8000 h^{-1}. At this temperature, only 48% of CO was converted when the contact time was 10 times less, 0.09 g s/cm^3 (NTP). At higher temperatures, the conversion of carbon monoxide to carbon dioxide eventually approaches the value dictated by the reaction equilibrium, e.g. 97% CO conversion at 527°C [38].

3.2.2. Effect of metal content

Fig. 5 shows WGS light-off curves over Cu–Ce(La)O_x catalysts with different copper contents from 5 to 40 at.%. Clearly, there is no appreciable difference in the light-off temperature of the reaction over these ceria-based catalysts, indicating that only a small amount of copper is adequate to change the WGS activity of ceria. A large excess of copper will form bulk CuO particles, which will have negligible interaction with ceria. However, the total number of highly dispersed copper clusters may also increase with copper loading. Hence, only a kinetic study will determine the effect of copper loading on the catalyst activity. We recently reported on such a study for similar type catalysts used in CO oxidation [22,24,45].

The effect of nickel content in Ni–Ce(La)O_x catalysts on the WGS light-off temperature was also examined [26]. The 5 at.% Ni–Ce(La)O_x sample, made by coprecipitation, showed a higher CO conversion to

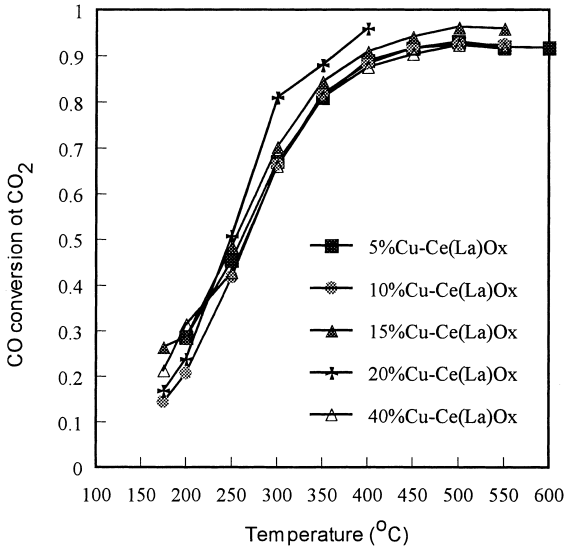

Fig. 5. Effect of copper content on the WGS activity of Cu–Ce(10% La)O_x, 2% CO–10.7% H_2O–He, S.V.=80 000 h^{-1} (NTP).

CO_2 than either of the higher nickel-content catalysts, 5 wt.% Ni–Ce(La)O_x and 7 wt.% Ni/Ce(La)O_x, which were prepared by incipient wetness impregnation of Ce(La)O_x (Table 1). Also, as shown in Fig. 1, there are differences between the light-off performance of Cu- and Ni-containing ceria catalysts, the former showing higher activity at temperatures below 300°C. This was further investigated in the kinetic study.

3.2.3. Effect of hydrogen and H_2O/CO ratio

Hydrogen is produced by the water-gas shift reaction and is also present in large amounts in many practical feed gas streams. The effect of addition of about 40% hydrogen into the feed gas mixture on the conversion of CO over the 5 at.% Cu–Ce(La)O_x catalyst was examined. As shown in Fig. 6, over a wide temperature window (200–350°C), hydrogen did not significantly suppress the reaction. Above ~350°C, however, we see a decrease in the CO conversion due to the lower equilibrium value at this high concentration of hydrogen. Indeed, the 69.4% conversion of CO to CO_2 at 450°C in the 40% H_2-containing gas mixture is very close to the equilibrium value of 70% [39], as can be seen in Fig. 6.

Two different gas mixtures, containing 2% CO–10.7% H_2O and 0.2% CO–1.5% H_2O in helium, are compared over the 5 at.% Cu–Ce(La)O_x at a

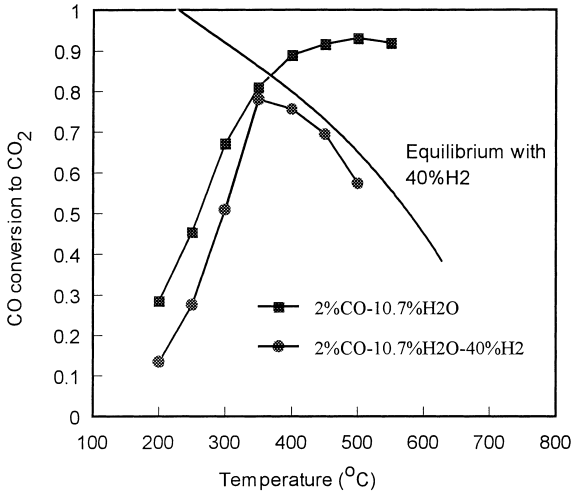

Fig. 6. Effect of hydrogen on the WGS activity of 5 at.% Cu–Ce(10% La)O_x, 2% CO–10.7% H_2O–He, S.V.=80 000 h^{-1} (NTP).

contact time of 0.9 g s/cc (NTP) in Fig. 7. In both gas streams, the conversion of carbon monoxide reached 90% above 200°C, while it was slightly higher for the 0.2% CO–1.5% H_2O gas mixture in the low temperature range. In this mixture, the molar ratio of H_2O/CO is higher (7.5:1) than in the other (5.3:1). In the literature, the H_2O content is crucial for the performance

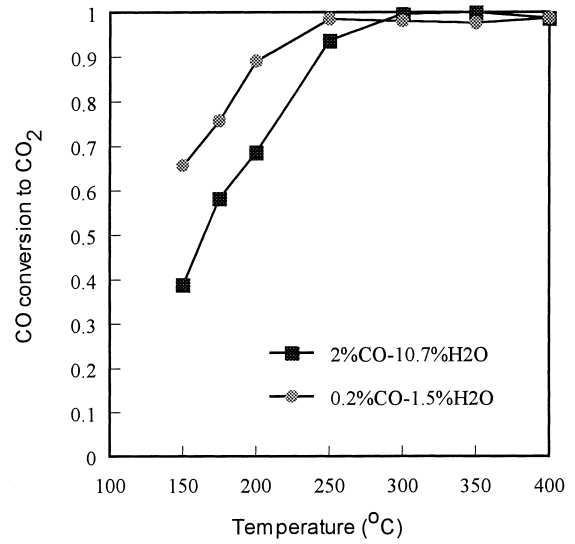

Fig. 7. Effect of H_2O/CO ratio on the conversion of CO to CO_2 in WGS over 5 at.% Cu–Ce(10% La)O_x, S.V.=8 000 h^{-1} (NTP).

of commercial CuO–ZnO catalysts [39–41]. The kinetics of the WGS reaction in H_2O-rich and CO-rich gases is considered below.

3.3. Kinetic studies

3.3.1. Water-gas shift reaction kinetics over Cu–Ce(La)O_x

Steady-state, water-gas shift kinetics was measured on the 5% Cu–Ce(La)O_x catalyst in the temperature range of 175–300°C. Reaction rates are shown in Fig. 8a as a function of P_{CO} at $P_{H_2O} = 0.02$ atm and in Fig. 8b as a function of P_{H_2O} at constant P_{CO}=0.02 atm. These and other kinetic data on this catalyst were best fitted by the redox model:

$$\text{Rate} = \frac{k_1 k_2 P_{CO} P_{H_2O}}{k_1 P_{CO} + k_2 P_{H_2O}}$$

Accordingly, in the limit of low P_{CO}/P_{H_2O}, the reaction is first order in CO and zeroth order in H_2O and vice versa for the other limiting case. The activation energy for the first case is 19.2 kJ/mol, while at high P_{CO}/P_{H_2O} the activation energy is 30.4 kJ/mol. Compared to the data of Fig. 8a, the WGS rate was 1.4–1.8 times higher on the 15 at.% Cu–Ce(La)O_x catalyst at 200°C [26]. Addition of copper into Ce(La)O_x significantly decreased the apparent activation energy of WGS over the latter, from 58.5 [26] to 30.4 kJ/mol, as can be seen in Table 2. Also, the Cu–ceria catalyst, prepared in this work, displays a several-fold lower activation energy than other reported Cu-catalysts, including some commercial Cu–ZnO catalysts (Table 2) [39,40].

We may extend the synergistic reaction model that we initially proposed for CO oxidation over Cu–CeO_2 composite catalyst by molecular O_2 and SO_2 [22–25,45] to the water-gas shift reaction, where the oxidant is now H_2O. Accordingly, CO molecules adsorbed on the copper clusters react with oxygen transported to the metal–ceria interface from ceria and water dissociates on an oxygen vacancy site of ceria [21] to H_2 and atomic oxygen, which re-oxidizes the ceria as shown in Fig. 9.

The overall reaction may be represented by the redox cycle:

$$H_2O + [\,]\text{-cat} \rightarrow H_2 + \text{O-cat}$$

$$\text{O-cat} + CO_{(a)} \rightarrow CO_2 + [\,]\text{-cat}$$

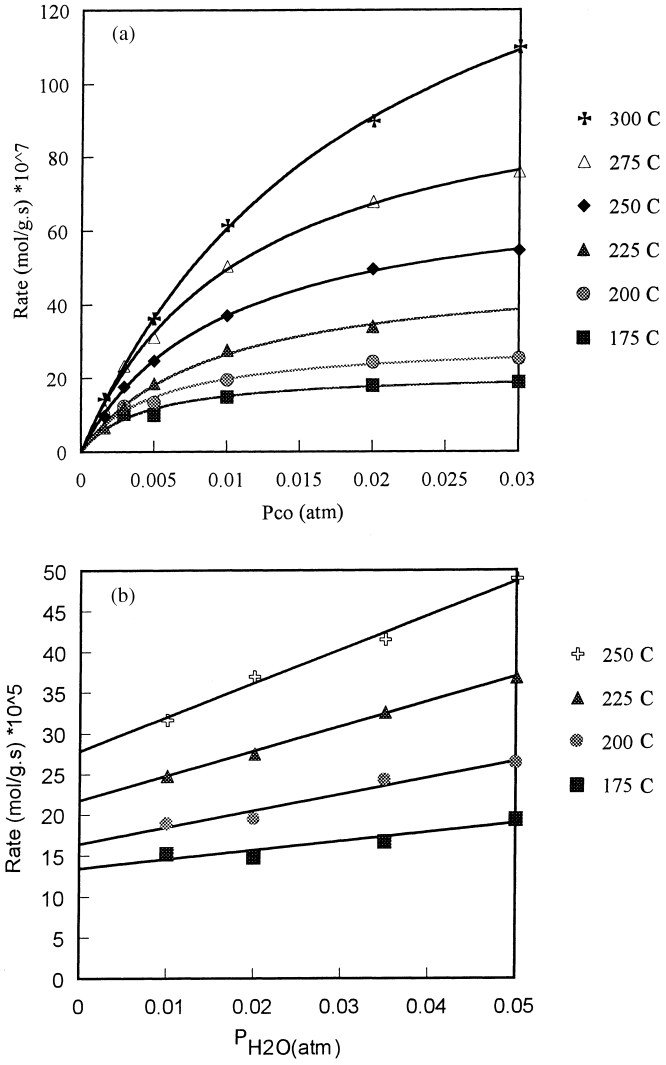

Fig. 8. (a) Variation of WGS rates with P_{CO} under constant P_{H_2O} = 0.02 atm; 5 at.% Cu–Ce(10% La)O_x, as-prepared; (b) variation of WGS rates with P_{H_2O} under constant P_{CO}=0.01 atm; 5 at.% Cu–Ce(10% La)O_x, as-prepared.

where $CO_{(a)}$ indicates carbon monoxide adsorbed on the metal cluster. We do not know the state of copper on ceria under WGS conditions. While a lot of evidence from the literature points out to metallic copper as the active phase in commercial Cu–ZnO catalysts [39], this has not been shown unambiguously. From our studies of the Cu–ceria system, all we can say with certainty is that bulk CuO particles, present in catalysts with high Cu content (>15 at.%), are reduced to metallic copper during reaction, as identified by XRD (Fig. 2). The copper clusters, which dominate at low Cu contents ($\leq$5 at.%), are XRD-silent. Yet, they are clearly visible by electron microscopy (STEM/EDS) [22,24,45]. These may contain Cu^+ sites at the interface with ceria [22,32]. Several other techniques, such as XPS, IR and UV–VIS, especially if performed in situ, may be combined to determine the oxidation state of Cu under WGS conditions.

As of now, there is no spectroscopic evidence of H_2O dissociation on the Cu–CeO_2 system, as implied

Table 2
Water-gas shift (WGS) reaction kinetics

Catalyst	Conditions	E_{app} (kJ/mol)	m[a]	n[a]
Ce(La)O_x[b]	375–475°C	58.5	–	–
5 at.% Cu–Ce(10% La)O_x[b]	175–300°C, CO/H_2O=1.5	30.4	0	1
	H_2O/CO=12.5	19.2	1	0
Cu (1 1 1) [34]	26 Torr CO–10 Torr H_2O, 612 K	71.1	0	0.5–1
Cu–Al_2O_3 [39]	180–220°C	59.3	1	1.9
Cu–ZnO–Al_2O_3 [39] (40% Cu, 22% Zn, 5% Al)	5 bar, 180–200°C	86.5	1	1.4
Cu–ZnO–Al_2O_3 [40]	267°C, H_2O/CO=0.38	41.8	0	1
ICI 52-1 [8]	250°C	–	1.08	0.55
CuO–MnO_2 [44]	229°C	55.0	1	1
Cu–ZnO–Cr_2O_3 [41]	300°C	112.0	–	–
5 at.% Ni–Ce(10% La)O_x[b]	275–300°C, CO/H_2O=1–1.5	38.2	0	1
5 wt.% Ni/Al_2O_3 [43]	250°C	78.2	−0.14	0.62

[a] m and n correspond to rate=$kP_{CO}^{m}P_{H_2O}^{n}$.
[b] This work.

by the redox mechanism above. The only such evidence in the literature comes from recent work of Kundakovic et al. [42] who used soft X-ray photoemission spectroscopy and TPD to show the dissociation of adsorbed water on Rh–CeO_2. This supports the hypothesis of the redox mechanism for WGS on the Rh–CeO_2 system advanced by Bunluesin and Gorte [21].

Compared to CuO–Al_2O_3 [39], Table 2, Cu-Ce(La)O_x has much faster WGS kinetics. This is again similar to what was reported for the Pt-metals on alumina versus ceria supports [21]. Thus, the co-operative effect between the metal and ceria in WGS may be displayed by a variety of transition metal–ceria systems at low temperatures. The copper-modified cerium oxide system is an attractive low-temperature water-gas shift catalyst also because of its high stability. As shown in Figs. 1 and 5–7 and Table 1, Cu–Ce(La)O_x maintains high reactivity and stability at high temperatures (up to 600°C).

3.3.2. Water-gas shift reaction kinetics over Ni–Ce(La)O_x

Fig. 10 shows measured rates of the water-gas shift reaction over the 5 at.% Ni–Ce(La)O_x catalyst, as a function of the partial pressure of CO at $P_{H_2O} = 0.02$ atm. These data were fitted by the redox model as for the Cu–ceria system above. At 300°C, the WGS rates are ∼1.5 times higher than those measured over Cu–ceria (Fig. 8a), while rates over the two catalysts are comparable at 275°C. However, at 250°C, the Ni–ceria system is much less active than Cu–Ce(La)O_x, especially at low P_{CO}/P_{H_2O}, Figs. 8a and 10. This is in agreement with the CO conversion data in Fig. 1. In view of the lower reducibility of NiO compared to CuO in the Ce(La)O_x matrix, Fig. 4, we may attribute the lower activity of Ni–Ce(La)O_x catalyst to the presence of NiO up to ∼275°C. Further work with pre-reduced catalysts is necessary to elucidate this point. Using the rate measurements at 275 and 300°C, Fig. 10, the apparent activation

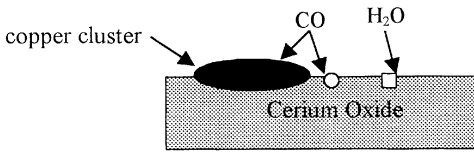

Fig. 9. Synergistic WGS reaction model.

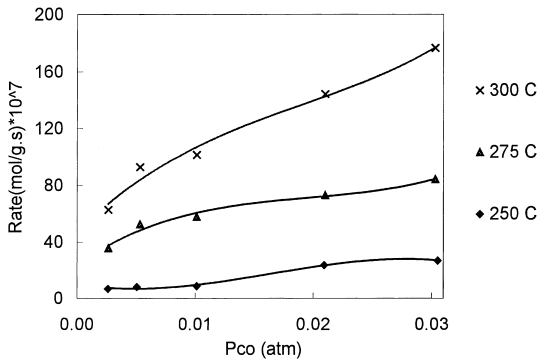

Fig. 10. Variation of WGS rates with P_{CO} under constant $P_{H_2O} = 0.02$ atm; 5 at.% Ni–Ce(10% La)O_x, as-prepared.

energy over Ni–ceria at CO-rich conditions was calculated to be 38.2 kJ/mol. This is close to the value of 30.4 kJ/mol calculated above for the Cu–ceria catalyst at CO-rich conditions, but using a wider temperature range, 175–300°C (Fig. 8a). Compared to 5 at.% Ni–Ce(La)O_x, a much higher WGS activation energy (78.2 kJ/mol) has been reported on 5 wt.% Ni–Al_2O_3 [43].

It is interesting that the apparent WGS activation energies for Cu and Ni–ceria catalysts reported here are not too different than the value of 46 kJ/mol reported by Bunluesin and Gorte [21] for Rh–ceria, Pd–ceria and Pt–ceria. The specific WGS rates on Rh–ceria were two-orders of magnitude higher than those on Rh–alumina. This was attributed to an enhanced redox mechanism on ceria which is absent on alumina. Indeed, this enhanced WGS rate correlates with the increased oxygen storage capacity (OSC) of ceria imparted by the platinum metal addition [18]. The improvement disappears if ceria is intentionally sintered to a state of low OSC [21]. The co-operative effect of Cu or Ni and ceria for the WGS reaction can also be discussed along the same lines.

4. Conclusions

Cu–Ce(La)O_x, Ni–Ce(La)O_x, as well as Ce(La)O_x, prepared in nanocrystalline form, were examined as WGS catalysts in this work. Copper and nickel oxide added in small amounts (2–3 wt.%) in ceria form clusters closely associated with the ceria surface. The activity of ceria for the water-gas shift reaction was significantly enhanced by the addition of the base metal. The largest effect was displayed by the copper-modified catalyst. The WGS activity correlates well with an enhanced reducibility of ceria, starting at below 200°C for Cu–Ce(La)O_x and below 300°C for the Ni–Ce(La)O_x material. High metal content, on the other hand, leads to bulk particle formation and negligible contribution to the catalyst activity.

Steady-state WGS kinetics were measured over the temperature range of 175–300 and 250–300°C, respectively, for Cu–Ce(La)O_x and Ni–Ce(La)O_x. The activation energy of the reaction over Ce(La)O_x was 58.5 kJ/mol, while it was 38.2 and 30.4 kJ/mol, respectively, over the 5 at.% Ni- and 5 at.% Cu–Ce(La)O_x catalysts in CO-rich conditions. A co-operative redox reaction mechanism, involving oxidation of CO adsorbed on the metal cluster by oxygen supplied to the metal interface by ceria, followed by H_2O filling of the oxygen vacancy on ceria, was used to fit the kinetics. Parametric studies were mainly performed with the 5 at.% Cu–(La)O_x catalyst. Hydrogen addition in the feed gas did not suppress the reaction. Notably, the Cu–ceria catalyst requires no activation and retains high WGS activity and stability at temperatures up to 600°C.

Acknowledgements

The financial support of this work by Reaction Engineering International under contract with NASA Grant No. NAS 2-97018 and the NSF/EPA support CTS-9985305 to one of us (Q. Fu) are gratefully acknowledged.

References

[1] M.I. Temkin, Adv. Catal. 28 (1979) 263.
[2] P.C. Ford, Acc. Chem. Res. 14 (1981) 31.
[3] D.S. Newsome, Catal. Rev. Sci. Eng. 21 (1980) 275.
[4] C. Rhodes, G.J. Huchings, A.M. Ward, Catal. Today 23 (1995) 43.
[5] A. Andreev, T. Halachev, D. Shopov, Izv. Khim. 21 (3) (1988).
[6] G.G. Shchibrya, A.M. Alekseev, R.V. Chesnokova, B.G. Lyudkovskaya, Kinet. Katal. 12 (1971) 1186.
[7] T.M. Yur'eva, G.K. Boreskov, V.Sh. Gruver, Kinet. Katal. 10 (1969) 294.
[8] T. Salmi, R. Hakkarainen, Appl. Catal. 49 (1989) 285–306.
[9] M.A. Segura, C.L. Aldridge, US Patent 4.054,644 (1977).
[10] H.J. Henkel, C. Koch, H. Kostka, German Patent 2,643,916 (1978).
[11] D. Andreeva, V. Idakiev, T. Tabakova, A. Andreev, R. Giovanoli, Appl. Catal. A: Gen. 134 (1996) 275–283.
[12] D. Andreeva, V. Idakiev, T. Tabakova, A. Andreev, R. Giovanoli, J. Catal. 158 (1996) 354–355.
[13] H. Sakurai, A. Ueda, T. Kobayashi, M. Haruta, Chem. Commun. (1997) 271–272.
[14] M. Haruta, Catal. Today 36 (1997) 153–166.
[15] G. Munuera, A. Aernandez, A.R. Gonzales-Elipe, Stud. Surf. Sci. Catal. 71 (1991) 207.
[16] D. Kalakkad, A.K. Datye, H. Robota, Appl. Catal. B: Environ. 1 (1992) 191.
[17] J.C. Schlatter, P.J. Mitchell, Ind. Eng. Chem. Prod. Res. Dev. 19 (1980) 288.
[18] H.C. Yao, Y.F.Y. Yao, J. Catal. 86 (1984) 254.
[19] H.S. Ghandi, A.G. Piken, M. Shelef, R.G. Deloch, SAE Paper 760201, 1976.

[20] M. Weibel, F. Garin, P. Bernhardt, G. Maire, M. Prigent, Catalysis and automotive pollution control II, in: Proceedings of the Second International Symposium, Studies in Surface Science and Catalysis, Vol. 71, 1991.
[21] T. Bunluesin, R.J. Gorte, Appl. Catal. B: Environ. 15 (1998) 107.
[22] W. Liu, Sc.D. Thesis, Massachusetts Institute of Technology, 1995.
[23] W. Liu, A.F. Sarofim, M. Flytzani-Stephanopoulos, Appl. Catal. B: Environ. 4 (1994) 167.
[24] W. Liu, M. Flytzani-Stephanopoulos, J. Catal. 153 (1995) 304–316.
[25] W. Liu, C. Wadia, M. Flytzani-Stephanopoulos, Catal. Today 28 (4) (1996) 391.
[26] Y. Li, M.S. Thesis, Department of Chemical Engineering, Tufts University, 1999.
[27] T. Zhu, Lj. Kundakovic, A. Dreher, M. Flytzani-Stephanopoulos, Catal. Today 50 (1999) 381–397.
[28] Y. Amenomiya, A. Emesh, K. Oliver, G. Pleizer, in: M. Philips, M. Ternan (Eds.), Proceedings of the Ninth International Congress Catal., Chemical Institute of Canada, Ottawa, Canada, 1988, p. 634.
[29] Lj. Kundakovic, Ph.D. Thesis, Department of Chemical Engineering, Tufts University, 1998.
[30] Lj. Kundakovic, M. Flytzani-Stephanopoulos, J. Catal. 179 (1998) 203–221.
[31] T. Zhu, A. Dreher, M. Flytzani-Stephanopoulos, Appl. Catal. B: Environ. 21 (1999) 103–120.
[32] C. Lamonier, A. Ponchel, A. D'Huysser, L. Jalowiecki-Duhamel, Catal. Today 50 (1999) 247.
[33] W. Liu, M. Flytzani-Stephanopoulos, Chem. Eng. J. 64 (1996) 283.
[34] J. Barrault, A. Alouche, V. Paul-Boncour, L. Hilaire, A. Percheron-Guegan, Appl. Catal. 46 (1989) 269–279.
[35] G. Fierro, M.L. Jacono, M. Inversi, P. Porta, R. Lavecchia, F. Cioci, J. Catal. 148 (1994) 709.
[36] A.L. Boyce, S.R. Graville, P.A. Sermon, M.S.W. Vong, React. Kinet. Catal. Lett. 434 (1) (1991) 1.
[37] L. Kundakovic, M. Flytzani-Stephanopoulos, Appl. Catal. A: Gen. 171 (1998) 13–29.
[38] R.F. Probstein, R.E. Hicks, Synthetic Fuels, McGraw-Hill, New York, 1976.
[39] C.V. Ovesen, B.S. Clausen, B.S. Hammershøi, G. Steffensen, T. Askgaard, I. Chorkendroff, J.K. Nørskov, P.B. Rasmussen, P. Stoltze, P. Taylor, J. Catal. 158 (1996) 170–180.
[40] M.J.L. Gines, N. Amadeo, M. Laborde, C.R. Apesteguia, Appl. Catal. A: Gen. 131 (1995) 283–296.
[41] E.M. Cherednik, N.M. Morozov, M.I. Temkin, Kinet. Katal. 10 (1969) 603.
[42] Lj. Kundakovic, D.R. Mullins, S.H. Overbury, Chemisorption and reaction of H_2O and CO on oxidized and reduced Rh/CeO_x surfaces, 1999 Annual AIChE Mtg., paper #284f, Dallas, TX, 31 October–5 November 1999.
[43] D.C. Grenoble, M.M. Estadt, D.F. Ollis, J. Catal. 67 (1981) 90.
[44] G.J. Hutchings, R.G. Copperthwaite, F.M. Gottschalk, R. Hunter, J. Mellor, S.W. Orchard, T. Sangiorgio, J. Catal. 137 (1992) 408–422.
[45] W. Liu, M. Flytzani-Stephanopoulos, J. Catal. 153 (1995) 317–332.
[46] M. Flytzani-Stephanopoulos, T. Zhu, Catalytic recovery of elemental sulfur from sulfur dioxide-laden gas streams, ACS Volume on Green Engineering and Processing, 1999, in press.